



Scanning the optical characteristics of lead-free cesium titanium bromide double perovskite nanocrystals

Chenxi Yu(于晨曦), Long Gao(高龙), Wentong Li(李文彤), Qian Wang(王倩), Meng Wang(王萌), and Jiaqi Zhang(张佳旗)[†]

Citation: Chin. Phys. B, 2022, 31 (5): 054218. DOI: 10.1088/1674-1056/ac5984

Journal homepage: <http://cpb.iphy.ac.cn>; <http://iopscience.iop.org/cpb>

What follows is a list of articles you may be interested in

Noncollinear phase-matching geometries in ultra-broadband quasi-parametric amplification

Ji Wang(王佶), Yanqing Zheng(郑燕青), and Yunlin Chen(陈云琳)

Chin. Phys. B, 2022, 31 (5): 054213. DOI: 10.1088/1674-1056/ac3a5b

Bandwidth-tunable silicon nitride microring resonators

Jiacheng Liu(刘嘉成), Chao Wu(吴超), Gongyu Xia(夏功榆), Qilin Zheng(郑骑林), Zhihong Zhu(朱志宏), and Ping Xu(徐平)

Chin. Phys. B, 2022, 31 (1): 014201. DOI: 10.1088/1674-1056/ac2e64

Propagations of Fresnel diffraction accelerating beam in Schrödinger equation with nonlocal nonlinearity

Yagang Zhang(张亚港), Yuheng Pei(裴宇恒), Yibo Yuan(袁一博), Feng Wen(问峰), Yuzong Gu(顾玉宗), and Zhenkun Wu(吴振坤)

Chin. Phys. B, 2021, 30 (11): 114209. DOI: 10.1088/1674-1056/ac068e

A low-threshold multiwavelength Brillouin fiber laser with double-frequency spacing based on a small-core fiber

Lu-Lu Xu(徐路路), Ying-Ying Wang(王莹莹), Li Jiang(江丽), Pei-Long Yang(杨佩龙), Lei Zhang(张磊), and Shi-Xun Dai(戴世勋)

Chin. Phys. B, 2021, 30 (8): 084210. DOI: 10.1088/1674-1056/abff47

Low-threshold bistable reflection assisted by oscillating wave interaction with Kerr nonlinear medium

Yingcong Zhang(张颖聪), Wenjuan Cai(蔡文娟), Xianping Wang(王贤平), Wen Yuan(袁文), Cheng Yin(殷澄), Jun Li(李俊), Haimei Luo(罗海梅), and Minghuang Sang(桑明煌)

Chin. Phys. B, 2021, 30 (8): 084203. DOI: 10.1088/1674-1056/abe118

Scanning the optical characteristics of lead-free cesium titanium bromide double perovskite nanocrystals

Chenxi Yu(于晨曦), Long Gao(高龙), Wentong Li(李文彤), Qian Wang(王倩),
Meng Wang(王萌), and Jiaqi Zhang(张佳旗)[†]

Key Laboratory of Automobile Materials, Ministry of Education, College of Materials Science and Engineering, Jilin University, Changchun 130012, China

(Received 28 December 2021; revised manuscript received 14 February 2022; accepted manuscript online 2 March 2022)

Cs₂TiBr₆ nanocrystals (NCs) are a type of promising optoelectronic materials, owing to their high photoelectric properties and non-toxicity. Here, we synthesize the colloidal Cs₂TiBr₆ NCs using a hot-injection approach. The temperature-dependent absorption data shows that its energy band changes about 30 meV with temperature, reflecting that its energy band structure is much stable. The excitation intensity-dependent transient absorption data confirms its linear absorption cross-sections and carrier recombination rate constants, involving monomolecular and bimolecular recombination, which are all superior to those of conventional perovskite bromide counterparts. In addition, its nonlinear absorption cross-sections are also measured based on femtosecond Z-scan. Our results suggest that Cs₂TiBr₆ NCs can be extensively applied in the field of optoelectronics, owing to its excellent carrier dynamics and nonlinear optical properties.

Keywords: Cs₂TiBr₆, nonlinear optics, ultrafast spectroscopy, absorption spectra

PACS: 42.65.-k, 78.47.J-, 78.40.Fy

DOI: 10.1088/1674-1056/ac5984

1. Introduction

Functional nanomaterials are of great importance for many applications.^[1,2] Recently, perovskite lead halides, a new type of semiconducting nanomaterials have exhibited a very fast development in photovoltaics,^[3] light-emitting diodes (LEDs),^[4] photocatalysis,^[5] lasers,^[6] photodetectors, *et al.*,^[7] due to their tuneable spectrum,^[8] strong photoluminescence,^[6] reasonable defect tolerance,^[9] high diffusion coefficient,^[10] high carrier mobility,^[11] and long carrier lifetime.^[12] However, the stability of perovskites and the toxicity of Pb currently are two major obstacles for the practical application of perovskites, which the community is trying to overcome.^[13–17] Currently, two main forms are being proposed to address the toxicity of Pb, one is to use a monovalent cation and a trivalent cation to replace two divalent lead ions ($B^{+} + B^{3+} \rightarrow 2Pb^{2+}$) to form double perovskite formula $A_2B^{+}B^{3+}X_6$ (e.g., Cs₂AgInCl₆^[18–20]), the other is to use a tetravalent cation and a vacancy to replace two divalent lead ions ($B^{4+} + \text{vacancy} \rightarrow 2Pb^{2+}$) to form vacancy-ordered perovskite derivative formula A_2BX_6 (e.g., Cs₂TiBr₆). Cs₂TiBr_xI_{6-x}, a perovskite derivative structure material, was firstly synthesized as powders in 2017,^[21] showing benign defect properties and tuneable bandgap from 1.02 eV to 1.78 eV. Later, Cs₂TiBr₆ was prepared as films for photovoltaic application, yet the efficiency obtained was only 3.3%.^[22] So the application of the related devices is still a major challenge. Therefore, the in-depth study of relevant characteristics is of much importance for further application. Till now, most researches of Cs₂TiBr₆ materials are focusing on the basic opti-

cal and structural properties, and mainly via Cs₂TiBr₆ powders and polycrystalline films.^[23,24] However, more profound investigation of photo-physical properties is also very important, for example, its nonlinear optical properties, carrier dynamics, and temperature-dependent energy state evolution, which will influence further application of Cs₂TiBr₆ materials in the field of optoelectronics.

In this work, we demonstrate the photo-physical properties based on multi-spectroscopy for lead-free double perovskite Cs₂TiBr₆ nanocrystals (NCs). The energy band structure of Cs₂TiBr₆ NCs changes a little with temperature decreasing. Furthermore, the carrier recombination in the Cs₂TiBr₆-NC films, involving monomolecular and bimolecular, has been further studied by TA technique. And the nonlinear optical properties of Cs₂TiBr₆-NCs are investigated and the TPA section is confirmed according to the excitation intensity-dependent Z-scan technique, which excludes the interference of the excitation intensity.

2. Results and discussion

In this work, Cs₂TiBr₆ NCs were synthesized via a hot-injection method. First, we investigated the morphology of NCs by transmission electron microscopy (TEM), exhibiting uniform, hexagonal shaped NCs with an average diameter of 13.5 ± 1.9 nm, as shown in Figs. 1(a) and 1(b). The uniform morphology of our Cs₂TiBr₆ NCs benefits from the precise control of the reacting temperature and modified synthesis route, compared with previous reports.^[25,26] The corresponding x-ray diffraction (XRD) patterns are given in Fig. 1(c),

[†]Corresponding author. E-mail: zhangjiaqi@jlu.edu.cn

showing (111), (220), (222), (400), (440), and (622) planes at 14.3° , 23.56° , 28.78° , 33.42° , 47.84° , and 56.84° , respectively, which is consistent with the previous report.^[23] In addition, the elemental distribution was investigated by energy dispersive x-ray (EDX) analysis, presenting that the atomic ratio of Cs:Ti:Br is 20.08:9.97:69.95, as shown in supporting information (SI) Table S1, which is approximate to the ideal proportion of 2:1:6. The chemical properties were further studied by the x-ray photoelectron spectroscopy (XPS). Titanium presents as +4 valence state (Fig. 1(e)), confirm-

ing by the Ti $2p_{1/2}$ and $2p_{3/2}$ peaks at 459 eV and 465 eV, respectively.^[27] The aforementioned results combine to reveal that the as-prepared NCs are Cs_2TiBr_6 . The schematic crystal structure of Cs_2TiBr_6 is shown in Fig. 1(f), in which the Ti^{4+} sites and vacancies are alternatively occupied showing ordered vacancies. And the $[\text{TiBr}_6]^{2-}$ octahedra was isolated thus the structure can also be considered as Ti-deficient OD perovskite.

To study the evolution of the energy band structure of Cs_2TiBr_6 NCs with temperature, the temperature-dependent absorption spectra of Cs_2TiBr_6 NCs are given in Fig. 2(a).

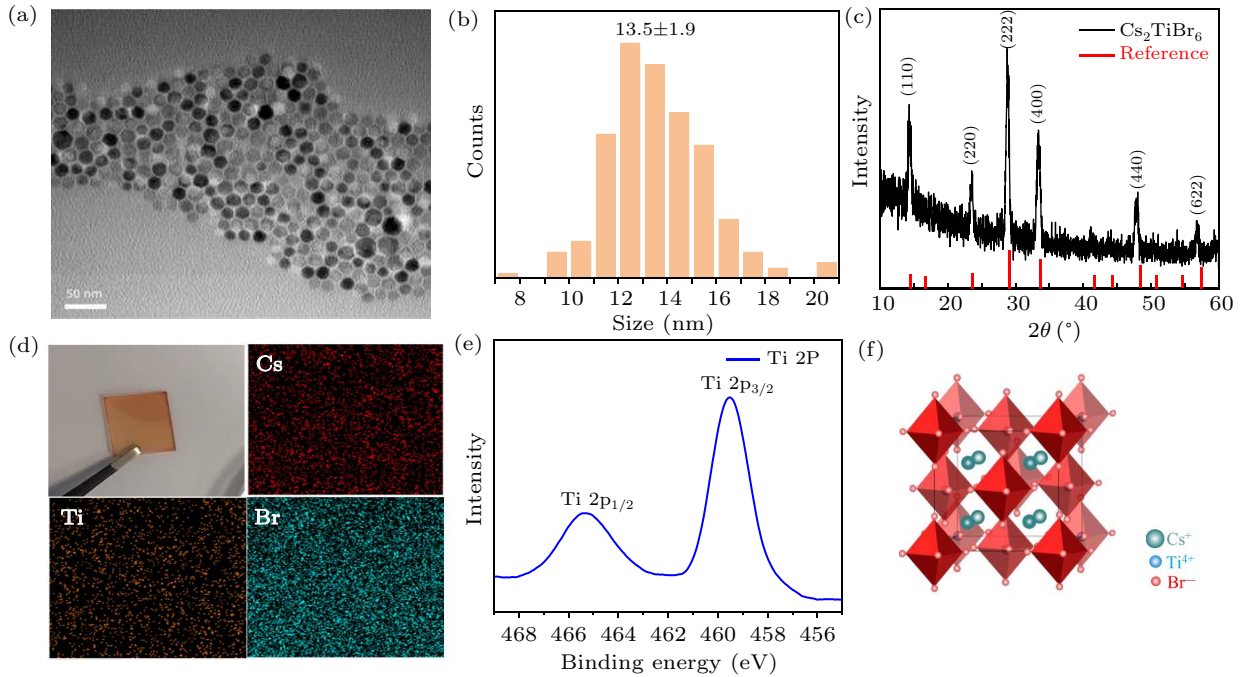


Fig. 1. (a) TEM image of Cs_2TiBr_6 NCs. (b) Size distribution histogram of Cs_2TiBr_6 NCs. (c) XRD patterns of Cs_2TiBr_6 NCs.^[23] (d) Digital photograph of Cs_2TiBr_6 NCs film and EDX elemental mapping of Cs_2TiBr_6 NCs. (e) XPS spectrum of Ti in Cs_2TiBr_6 NCs. (f) Schematic crystal structure of Cs_2TiBr_6 .

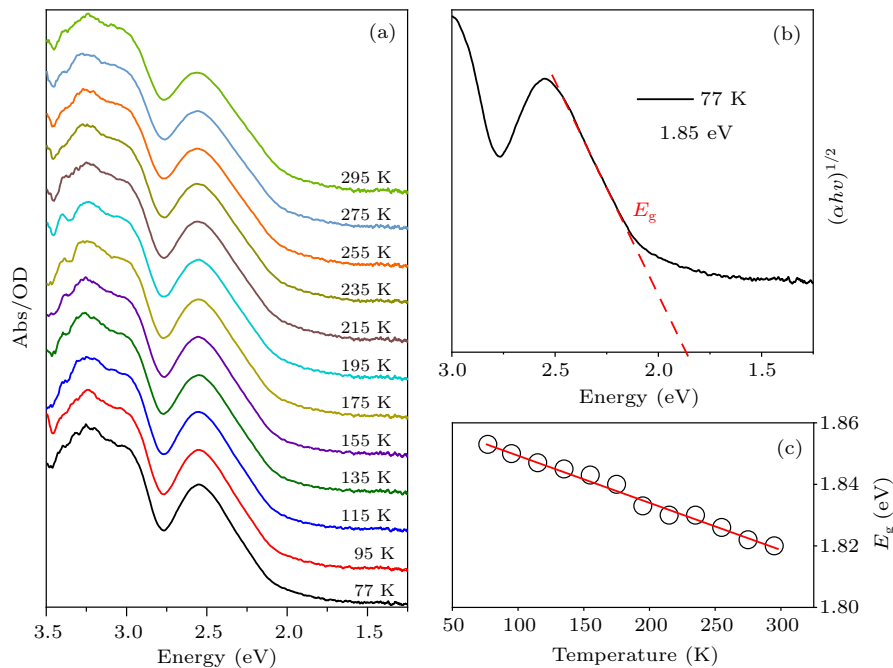


Fig. 2. (a) The temperature-dependent absorption spectra of Cs_2TiBr_6 NCs. (b) Tauc plot of Cs_2TiBr_6 NCs. (c) The changing of band edges of Cs_2TiBr_6 NCs with temperature increasing from 77 K to 295 K.

The shape of absorption spectra is almost invariable with the temperature decreasing, but the band edge shifts a little to the low-energy region simultaneously. As seen in Fig. 2(b), the bandgap of Cs₂TiBr₆ NCs can be estimated based on Tauc plots with indirect bandgap type. The E_g value is about 1.85 eV at 77 K and about 1.82 eV at 295 K. Compared to the previous reports about Cs₂TiBr₆ bulk powers and polycrystalline films, our NCs have similar bandgap at room temperature.^[21,28] Thus our Cs₂TiBr₆ NCs with a size of 13 nm are considered to have a negligible quantum effect. The band edges of Cs₂TiBr₆ NCs as a function of temperature are summarized in Fig. 2(c), showing that all of them almost linearly shift to the low energy region as the temperature lowers from 295 K to 77 K. As the temperature was varied about 220 K, the bandgap changes about 30 meV, implying that the energy band structure is almost invariable.

Actually, the intrinsic absorption properties of Cs₂TiBr₆ NCs can also be investigated by femtosecond transient absorption (fs-TA) spectroscopy techniques.^[29,30] Herein, figure 3(a) shows the time-dependent TA spectrum of Cs₂TiBr₆ NCs at room temperature, in which a strong ground state bleaching (GSB) signal is located at ~481 nm, meanwhile two photo-induced absorption (PIA) bands are located at 575 nm and 448 nm, respectively. The PIA signal at 575 nm narrows noticeably with time prolonging in the low energy region, compared to the GSB signal, where the change is less obvious. Figure 3(b) shows the TA spectrum of Cs₂TiBr₆ NCs at 77 K, which is also composed of a small PIA at 440 nm, a GSB at 493 nm and a PIA at 560 nm. Apparently, the shift of the signal is assigned to the variance of the energy structure.

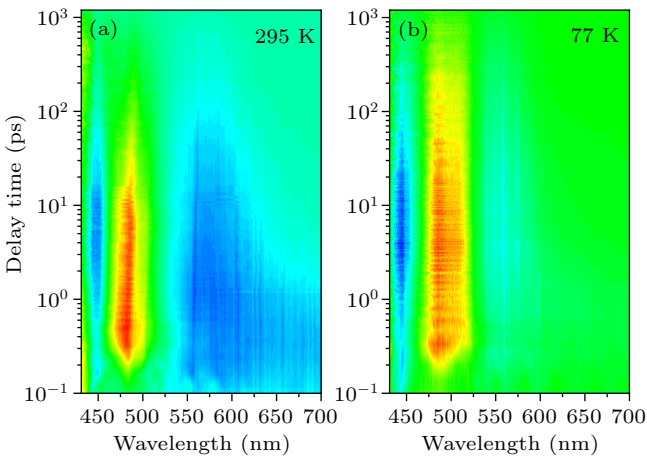


Fig. 3. The time-dependent TA spectra of Cs₂TiBr₆ NCs (a) at room temperature and (b) at 77 K.

Considering that Cs₂TiBr₆ NCs have a huge potential in the optoelectronic field,^[31] the understanding of carrier recombination dynamics is of much importance.^[32] The TA curves of Cs₂TiBr₆ NCs as a function of excitation intensity were probed at room temperature and 77 K (as seen in Figs. 4(a) and 4(b)). Herein, the Cs₂TiBr₆ NC films in our experiment were all prepared by drop-casting on a glass

substrate and subsequently permitting the solvent evaporation at room temperature under inert gas environment.^[33] The pump flux-dependent bleaching signal of Cs₂TiBr₆ NCs at room temperature and 77 K is given in Figs. 4(c) and 4(d). Based on Poisson statistics,^[34] the absorption cross sections of these Cs₂TiBr₆ NCs at 400 nm can be extracted, which are $3.74 \times 10^{-13} \text{ cm}^2$ at room temperature and $5.60 \times 10^{-13} \text{ cm}^2$ at 77 K. Apparently, the absorption coefficient was enhanced with the temperature decreasing. Compared with lead halide perovskite (MAPbBr₃), the absorption cross section is one order of magnitude higher.^[35] Simultaneously, Cs₂TiBr₆ NCs process a higher absorption coefficient than double perovskite Cs₂AgIn_xBi_{1-x}Cl₆ ($x = 0, 0.75$) and Cs₂AgSb_{0.25}Bi_{0.75}Br₆ NCs are much better than CsPbBr₃ perovskites.^[36-41] Note that the GSB curve only exhibits a simple exponential relaxation behavior at low excitation intensity when the temperature is 295 K (room temperature). After the pump fluence exceeds $4.08 \times 10^{13} \text{ photon}\cdot\text{cm}^{-2}$, an excitation intensity-dependent rapid relaxation component gradually appears in the GSB curves, causing the GSB curves exhibiting an apparent multi-exponential relaxation behavior. Moreover, its weight seems to enhance with the excitation intensity.^[42-46] The similar phenomenon was observed at 77 K. Based on the analysis of TA data, it is found that the recombination rate constants can be quantitatively ascertained by employing the polynomial rate equation^[32]

$$\frac{dn}{dt} = -k_1n - k_2n^2, \quad (1)$$

where n denotes the initial carrier density; k_1 and k_2 are the monomolecular and bimolecular recombination rate constants, respectively. In other words, the Auger recombination process did not appear in the GSB curves, even though the intensity has increased to $13.41 \times 10^{13} \text{ photon}\cdot\text{cm}^{-2}$. This suggests that the carrier diffusion velocity in Cs₂TiBr₆ NCs film is really rapid, which can restrict the happening of Auger recombination. After fitting, these recombination rate constants of Cs₂TiBr₆ NCs can be extracted from the excitation intensity-dependent TA curves and summarized in Figs. 4(c) and 4(d). As the temperature decreases to 77 K, the monomolecular recombination constant k_1 apparently decreases from $9.5 \times 10^9 \text{ s}^{-1}$ to $6.2 \times 10^9 \text{ s}^{-1}$, meanwhile the bimolecular recombination constant k_2 increases from $0.9 \times 10^{-9} \text{ cm}^3\cdot\text{s}^{-1}$ to $3.1 \times 10^{-9} \text{ cm}^3\cdot\text{s}^{-1}$. Generally speaking, k_2 of Cs₂TiBr₆ NCs film is smaller in comparison with other conventional perovskite materials,^[19,45,47,48] suggesting that the loss originated from bimolecular recombination in devices based on Cs₂TiBr₆ NCs should be less than that based on other perovskite materials. According to the previous report,^[49] the thermally activated charge trapping model can be responsible for this phenomenon. As the temperature decreases, the activity of carriers gradually weakens, compelling the carriers to spend much time overcoming the energy barrier and recombining with the

shallow defects. In this situation, the monomolecular recombination constant has to decrease with temperature dropping. Meanwhile, the carriers left in the intra-band apparently increase, which enhances the bimolecular recombination constant. Moreover, the decreasing temperature can lead to the shrinkage of the lattice and up shift the distribution of defects,

which restricts the capture of carriers originated from the defects. This can also restrict the monomolecular recombination. On the other hand, the decreasing temperature restricts the vibration of the lattice and weakens the carrier-phonon scattering, which facilitates the migration of carriers and accelerates the monomolecular recombination simultaneously.

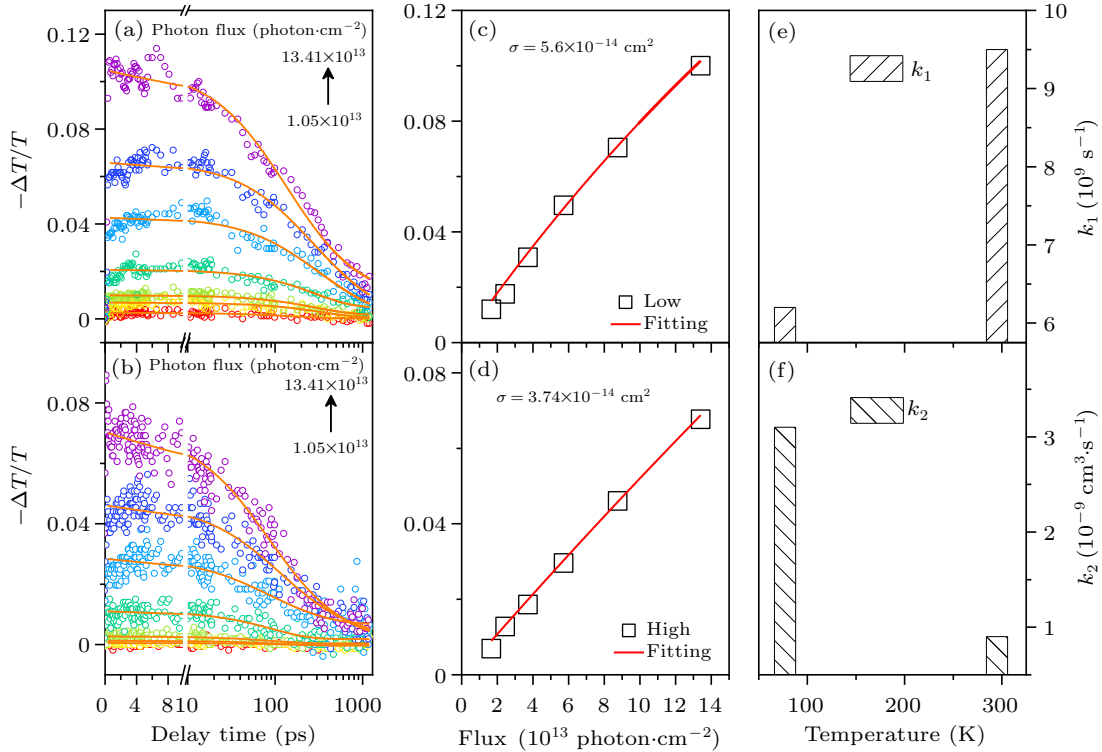


Fig. 4. The Cs₂TiBr₆ NCs TA (dynamic) curves with excitation at 480 nm at room temperature (a) and 77 K (b). The pump flux-dependent bleaching peak of Cs₂TiBr₆ NCs at room temperature (c) and 77 K (d). The monomolecular and bimolecular recombination rate constants (e) k_1 and (f) k_2 .

Besides the temperature-dependent energy band and carrier properties, the traditional perovskite NCs often exhibit excellent two-photon absorption (TPA) properties and have a huge potential in the field of conventional electronic switches.^[50] Herein, the TPA properties of Cs₂TiBr₆ NCs were measured by excitation intensity-dependent open-hole Z-scan technique,^[51,52] as shown in Fig. 5, showing that the valley of Cs₂TiBr₆ NCs is estimated to be 1.34×10^{-3} M, according to the linear absorption coefficient. The scattered data and systematic asymmetry in baselines are usually caused by laser instability and surface imperfection and can be corrected by the low intensity background responses. Moreover, the contribution from the solvent has been excluded in our experiment. The obtained data clearly indicates a reverse saturable absorption type of behavior and the depth of valley is apparently enhanced with the excitation intensity. By fitting the Z-scan curves, the two-photon absorption coefficients (β) of Cs₂TiBr₆ NCs were measured and shown as the inset of Fig. 5, which is almost independent of the excitation intensity. Finally, the two-photon absorption (TPA) cross section (σ_{TAP}) of Cs₂TiBr₆ NCs is estimated to be 1070 GM, which is apparently larger than that of other typical perovskite bromide

materials.^[53] Apparently, Cs₂TiBr₆ NCs can provide broad bandwidth unattainable by conventional electronic switches owing to their nonlinear optical properties.

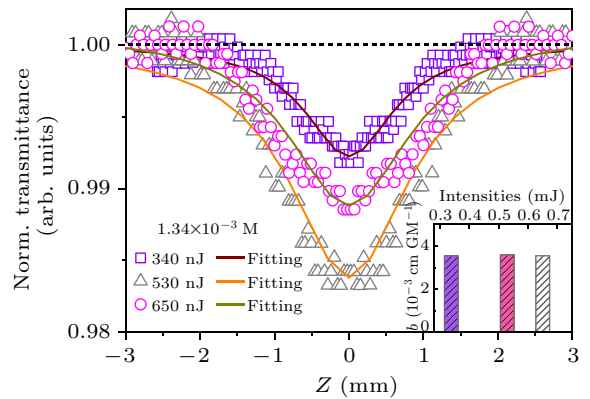


Fig. 5. Excitation intensity dependent Z-scan curves of Cs₂TiBr₆ NCs. Inset: β at different excitation intensity.

3. Conclusion and perspectives

In summary, we report on the synthesis of lead-free double perovskite Cs₂TiBr₆ NCs and confirm its photo-physical properties based on multi-spectroscopy. It is interesting to find

that the energy band structure of Cs₂TiBr₆ NCs changes a little with temperature decreasing. In addition, the carrier recombination, involving monomolecular and bimolecular, occurring in the Cs₂TiBr₆·NC films has been further investigated by TA technique, indicating that the monomolecular recombination decreases with the temperature lowering, yet the bimolecular recombination shows opposite tendency. Moreover, the nonlinear optical properties of Cs₂TiBr₆·NC are studied and its TPA section is estimated to be 1070 GM based on the excitation intensity-dependent Z-scan technique, which excludes the interference of excitation intensity. This provides a comprehensive insight into the photo-physical properties of double perovskite NCs, suggesting that this type of perovskite nanomaterials have great potential in the fields of conventional electronic switches.

Acknowledgements

Project supported by the National Natural Science Foundation of China (Grant No. 61804063) and the Natural Science Foundation of Jilin Province, China (Grant No. 20190201208JC).

References

- Cao Z, Hu F, Man Z, Zhang C, Zhang W, Wang X and Xiao M 2020 *Chin. Phys. Lett.* **37** 1
- Li L, Bao Z L, Ye X H, Shen J W, Yang B, Ye G X and Tao X M 2020 *Chin. Phys. Lett.* **37** 028102
- Min H, Lee D Y, Kim J, Kim G, Lee K S, Kim J, Paik M J, Kim Y K, Kim K S, Kim M G, Shin T J and Il Seok S 2021 *Nature* **598** 444
- Hassan Y, Park J H, Crawford M L, Sadhanala A, Lee J, Sadighian J C, Mosconi E, Shivanna R, Radicchi E, Jeong M, Yang C, Choi H, Park S H, Song M H, De Angelis F, Wong C Y, Friend R H, Lee B R and Snaith H J 2021 *Nature* **591** 72
- Chen Z, Hu Y, Wang J, Shen Q, Zhang Y, Ding C, Bai Y, Jiang G, Li Z and Gaponik N 2020 *Chem. Mater.* **32** 1517
- Dutta A, Behera R K, Pal P, Baitalik S and Pradhan N 2019 *Angew. Chemie* **131** 5608
- Shen K, Xu H, Li X, Guo J, Sathasivam S, Wang M, Ren A, Choy K L, Parkin I P, Guo Z and Wu J 2020 *Adv. Mater.* **32** 2000004
- Jiang Y, Cui M, Li S, Sun C, Huang Y, Wei J, Zhang L, Lv M, Qin C, Liu Y and Yuan M 2021 *Nat. Commun.* **12** 1
- Chu W, Zheng Q, Prezhdo O V, Zhao J and Saidi W A 2020 *Sci. Adv.* **6** eaaw7453
- Zhumekenov A A, Saidaminov M I, Haque M A, Alarousu E, Sarmah S P, Murali B, Dursun I, Miao X H, Abdelhady A L, Wu T, Mohammed O F and Bakr O M 2016 *ACS Energy Lett.* **1** 32
- Turren-Cruz S H, Saliba M, Mayer M T, Juárez-Santesteban H, Mathew X, Nienhaus L, Tress W, Erodici M P, Sher M J, Bawendi M G, Grätzel M, Abate A, Hagfeldt A and Correa-Baena J P 2018 *Energy Environ. Sci.* **11** 78
- Shi E, Gao Y, Finkenauer B P, Akriti A, Coffey A H and Dou L 2018 *Chem. Soc. Rev.* **47** 6046
- Creutz S E, Crites E N, De Siena M C and Gamelin D R 2018 *Nano Lett.* **18** 1118
- Yang B, Chen J, Yang S, Hong F, Sun L, Han P, Pullerits T, Deng W and Han K 2018 *Angew. Chemie - Int. Ed.* **57** 5359
- Lee W, Choi D and Kim S 2020 *Chem. Mater.* **32** 6864
- Han P, Mao X, Yang S, Zhang F, Yang B, Wei D, Deng W and Han K 2019 *Angew. Chemie - Int. Ed.* **58** 17231
- Slavney A H, Hu T, Lindenberg A M and Karunadasa H I 2016 *J. Am. Chem. Soc.* **138** 2138
- Liu Y, Rong X, Li M, Molokeev M S, Zhao J and Xia Z 2020 *Angew. Chemie - Int. Ed.* **59** 11634
- Chen Z, Li Z, Zhang C, Jiang X F, Chen D, Xue Q, Liu M, Su S, Yip H L and Cao Y 2018 *Adv. Mater.* **30** 1801370
- Liu Y, Nag A, Manna L and Xia Z 2021 *Angew. Chemie - Int. Ed.* **60** 11592
- Ju M G, Chen M, Zhou Y, Garces H F, Dai J, Ma L, Padture N P and Zeng X C 2018 *ACS Energy Lett.* **3** 297
- Chen M, Ju M G, Carl A D, Zong Y, Grimm R L, Gu J, Zeng X C, Zhou Y and Padture N P 2018 *Joule* **2** 558
- Kong D, Cheng D, Wang X, Zhang K, Wang H, Liu K, Li H, Sheng X and Yin L 2020 *J. Mater. Chem. C* **8** 1591
- Euvarard J, Wang X, Li T, Yan Y and Mitzi D B 2020 *J. Mater. Chem. A* **8** 4049
- Liga S M and Konstantatos G 2021 *J. Mater. Chem. C* **9** 11098
- Grandhi G K, Matuhina A, Liu M, Annurakshita S, Ali-Löyty H, Bautista G and Vivo P 2021 *Nanomaterials* **11** 1458
- Mendes J L, Gao W, Martin J L, Carl A D, Deskins N A, Granados-Focil S and Grimm R L 2020 *J. Phys. Chem. C* **124** 24289
- Chen M, Ju M G, Carl A D, Zong Y, Grimm R L, Gu J, Zeng X C, Zhou Y and Padture N P 2018 *Joule* **2** 558
- Wang W, Sui N, Chi X, Kang Z, Zhou Q, Li L, Zhang H, Gao J and Wang Y 2021 *J. Phys. Chem. Lett.* **12** 861
- Wang X D, Miao N H, Liao J F, Li W Q, Xie Y, Chen J, Sun Z M, Chen H Y and Kuang D Bin 2019 *Nanoscale* **11** 5180
- Yang X, Wang W, Ran R, Zhou W and Shao Z 2020 *Energy and Fuels* **34** 10513
- Johnston M B and Herz L M 2016 *Acc. Chem. Res.* **49** 146
- P. P A, Joshi M, Verma D, Jadhav S, Choudhury A R and Jana D 2021 *ACS Appl. Nano Mater.* **4** 1305
- Chen J, Messing M E, Zheng K and Pullerits T 2019 *J. Am. Chem. Soc.* **141** 3532
- Zhang Y, Lou X, Chi X, Wang Q, Sui N, Kang Z, Zhou Q, Zhang H, Li L and Wang Y 2021 *J. Lumin.* **239** 118332
- Milot R L, Sutton R J, Eperon G E, Haghghirad A A, Martinez Hardigree J, Miranda L, Snaith H J, Johnston M B and Herz L M 2016 *Nano Lett.* **16** 7001
- Chen J, Židek K, Chábera P, Liu D, Cheng P, Nuutila L, Al-Marri M J, Lehtivuori H, Messing M E, Han K, Zheng K and Pullerits T 2017 *J. Phys. Chem. Lett.* **8** 2316
- Yang B, Mao X, Hong F, Meng W, Tang Y, Xia X, Yang S, Deng W and Han K 2018 *J. Am. Chem. Soc.* **140** 17001
- Nakahara S, Ohara K, Tahara H, Yumoto G, Kawawaki T, Saruyama M, Sato R, Teranishi T and Kanemitsu Y 2019 *J. Phys. Chem. Lett.* **10** 4731
- Yang B and Han K 2019 *Acc. Chem. Res.* **52** 3188
- Zhang F, Liu Y, Wei S, Chen J, Zhou Y, He R, Pullerits T and Zheng K 2021 *Sci. China Mater.* **64** 1418
- Milot R L, Eperon G E, Snaith H J, Johnston M B and Herz L M 2015 *Adv. Funct. Mater.* **25** 6218
- Wehrenfennig C, Liu M, Snaith H J, Johnston M B and Herz L M 2014 *Energy Environ. Sci.* **7** 2269
- Herz L M 2016 *Annu. Rev. Phys. Chem.* **67** 65
- Rehman W, Milot R L, Eperon G E, Wehrenfennig C, Boland J L, Snaith H J, Johnston M B and Herz L M 2015 *Adv. Mater.* **27** 7938
- Parrott E S, Green T, Milot R L, Johnston M B, Snaith H J and Herz L M 2018 *Adv. Funct. Mater.* **28** 1802803
- Ganesh N, Ghorai A, Krishnamurthy S, Banerjee S, Narasimhan K L, Ogale S B and Narayan K S 2020 *Phys. Rev. Mater.* **4** 084602
- Peters J A, Liu Z, Yu R, McCall K M, He Y, Kanatzidis M G and Wesels B W 2019 *Phys. Rev. B* **100** 1
- Zhang W, Yang F, Messing M E, Mergenthaler K, Pistol M E, Depert K, Samuelson L, Magnusson M H and Yartsev A 2016 *Nanotechnology* **27** 1
- Liang W Y, Liu F, Lu Y J, Popović J, Djurišić A and Ahn H 2020 *Opt. Express* **28** 24919
- Shen W, Chen J, Wu J, Li X and Zeng H 2021 *ACS Photonics* **8** 113
- Wei K, Xu Z, Chen R, Zheng X, Cheng X and Jiang T 2016 *Opt. Lett.* **41** 3821
- Espinosa D, Gonçalves E S and Figueiredo Neto A M 2017 *J. Appl. Phys.* **121** 043103